ELSEVIER

Journal of Nuclear Materials 307–311 (2002) 527–531

journal of nuclear materials

www.elsevier.com/locate/jnucmat

Comparison of in-beam fatigue behavior between austenitic and ferritic steels at 60 °C

Y. Murase [a], Johsei Nagakawa [a,b,*], N. Yamamoto [a]

[a] National Institute for Materials Science (NIMS), 1-2-1, Sengen, Tsukuba, Ibaraki 305-0047, Japan

[b] Interdisciplinary Graduate School of Engineering Sciences, Kyushu University, 6-1 Kasuga Koen, Kasuga, Fukuoka 816-8580, Japan

Abstract

Fatigue response was investigated for both 20% cold-worked 316 (316CW) austenitic stainless steel and F82H ferritic steel under 17 MeV proton irradiation at 60 °C. The loading mode was stress-controlled and tension–tension with two different loading ratios, $R = 0.44$ and 0.2 for both steels. The number of cycles to fracture (N_f) increased substantially under irradiation for both steels at $R = 0.44$, while the increase of N_f in the in-beam specimens disappeared for both steels at $R = 0.2$. Although the actual fatigue lifetime was generally similar in the unirradiated specimens of 316CW steels at $R = 0.44$ and F82H steel at $R = 0.2$, the prolongation of the lifetime under irradiation was detected only for 316CW steel at the respective loading mode. In this study, the dynamic irradiation effect on fatigue response will be discussed with respect to its dependence on the loading ratio (R) and the crystal structure (fcc/bcc).

1. Introduction

Austenitic stainless steels have many achievements on their excellent performances as structure materials for conventional type reactors, and are planned to be used in the experimental fusion reactor. However, in the recent decade, the main focus on the development of fusion reactor materials has shifted from austenitic stainless steels towards ferritic/martensitic stainless steels in the light of material design for a commercial fusion reactor. Since the accumulated displacement damage on the first wall of a commercial fusion reactor is estimated to reach more than 100 dpa, the use of austenitic steels is limited due to dimensional changes caused by severe void swelling [1]. Ferritic/martensitic steels have several advantages based on their resistance to void swelling, good thermal conductivity, low thermal expansion and well-established commercial production and fabrication technologies. A low activation ferritic/martensitic F82H steel has been developed for fusion applications by restricting alloying elements that produce long-lived radioactive isotopes through the nuclear reaction with high-energy neutrons [2]. This steel has been selected as one of the reference steels for the IEA round robin test on low activation ferritic steels, and extensive efforts have been made to characterize this steel and to accumulate data on a wide range of material properties [3].

In the thermonuclear fusion reactors of the tokamak-type, structure materials will receive not only severe atomic displacement damage but also various external loadings such as thermal and magnetic stresses, simultaneously. Since the nature of external loadings includes cyclic behaviour due to periodic operation of fusion reactors, it is important to understand the in-beam fatigue response of the material in order to evaluate its feasibility for fusion reactor applications. Although inadequate data have been accumulated due to some economical and technical difficulties in establishing the in-beam testing system, some workers have indicated evidences of dynamic irradiation effect on fatigue response of austenitic 316 type stainless steels [4–7].

In the present study, stress-controlled fatigue tests in tension–tension were performed for 20% cold-worked 316 stainless steel (316CW) and F82H steel under in situ irradiation with 17 MeV protons at 60 °C. The loading mode was triangular wave with two different loading

* Corresponding author.
E-mail address: yoshiharu.murase@nims.go.jp (Y. Murase).

0022-3115/02/$ - see front matter © 2002 Elsevier Science B.V. All rights reserved.
PII: S0022-3115(02)01212-6

Table 1
Chemical composition of 316CW and F82H steels (wt%)

	C	Ni	Cr	Mn	Mo	Si	P	S	V	W	Ta	Fe
316CW	0.06	10.30	16.79	1.17	2.16	0.68	0.027	0.001	–	–	–	Balance
F82H	0.09	0.02	7.82	0.1	0.003	0.07	0.001	–	0.19	1.98	0.004	Balance

ratios; R(max. load/min. load) = 0.44 and 0.2 for both steels. After the fatigue tests, the fracture surface was examined by scanning electron microscopy (SEM) for all specimens. The objective of the present study is to understand the dynamic irradiation effect on fatigue response with respect to its dependence on the applied loading ratio and the difference in crystal structure between 316CW (fcc) and F82H (bcc) steels.

2. Experimental procedure

The chemical compositions of 316 stainless steel and F82H steel are given in Table 1. Cold-rolled sheets of a commercial 316 stainless steel with a thickness of 0.19 mm were annealed for 30 min at 950 °C to obtain grain sizes <10 μm in diameter. The annealed sheets were further rolled to 20% reduction in thickness to produce the cold-worked sheets followed by the punching-out of fatigue specimens (316CW), as shown in Fig. 1. The specimen size was $4 \times 10 \times 0.15$ mm^3 in the gauge with a fatigue crack starter side-notch of 0.60 mm in length and 0.12 mm in width. The other material used in the present study was prepared from a 5 ton heat of F82H steel (IEA heat). The material sheets with a thickness of 2 mm were sliced from an industrial bulk stock by spark cutting and process-annealed at 780 °C for 30 min. The sheets were cold-rolled to 0.15 mm in thickness and punched out into the shape shown in Fig. 1. A side-notch was introduced into the gauge in the same way as that in the case of 316CW specimens. Final heat treatments for the F82H specimens were carried out at 940 °C for 30 min (normalizing) and at 750 °C for 60 min (tempering). These treatments yielded a fully martensitic structure with average austenitic grain size of 19 μm in diameter. Atomic displacement damage was introduced into both 316CW and F82H specimens with 17 MeV protons. The variation of the displacement damage rate between the two surfaces estimated by the SRIM 96 code was less than ±11%) and ±10% in the specimen thickness of 150 μm for 316CW and F82H steels, respectively. The atomic displacement damage rate was 1×10^{-7} dpa/s in the middle area of the specimen thickness. The specimen was cooled by a He gas jet in order to compensate the beam heating. The irradiation temperature was controlled to be (60 ± 3) °C by adjusting the helium gas flow to about 60 m/s. The temperature of the helium gas jet was 24 °C in the in-beam condition, the helium gas jet was warmed by electric heating to keep the specimen temperature of 60 °C under unirradiated conditions. Two pairs of chromel–alumel thermocouples were attached directly to the gauge by spot welding to monitor the specimen temperature. The two attaching points (upper and lower) were 2 mm away from the expected crack propagation path, so that the spot welding would not affect the fatigue process. Details of the in-beam fatigue testing machine and specimen installation have been described elsewhere [6].

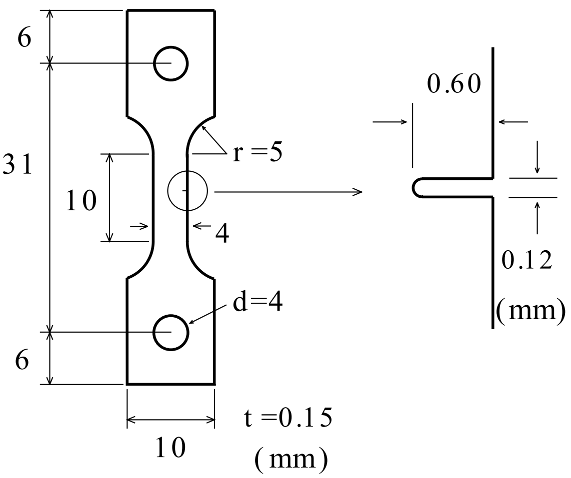

Fig. 1. Specimen type for the present fatigue experiments.

The loading mode was triangular and stress-controlled with two different loading ratios, $R = 0.44$ and 0.2 for both steels. The maximum applied stress in the loading mode should be lower than the yield stress at the notched ligament in order to avoid general yielding of the specimen [8]. The yield stress was 700 and 490 MPa for the specimen without a side-notch for 316CW and F82H steels, respectively. Therefore, the maximum nominal applied stresses were arranged to be 536.4 and 375 MPa, corresponding to 90% of the yield stresses at the ligament of 316CW and F82H specimens, respectively. Since the maximum applied stress was constant for each steel, the minimum stress was differently arranged for the two different loading ratios, $R = 0.44$ and 0.2. Fig. 2 shows the applied loading modes for (a) 316CW and (b) F82H specimens at $R = 0.44$ and 0.2 with descriptions of maximum–minimum loading stress, load changing rate, average loading stress (σ_m) and loading stress amplitude (σ_a) in each diagram. After the

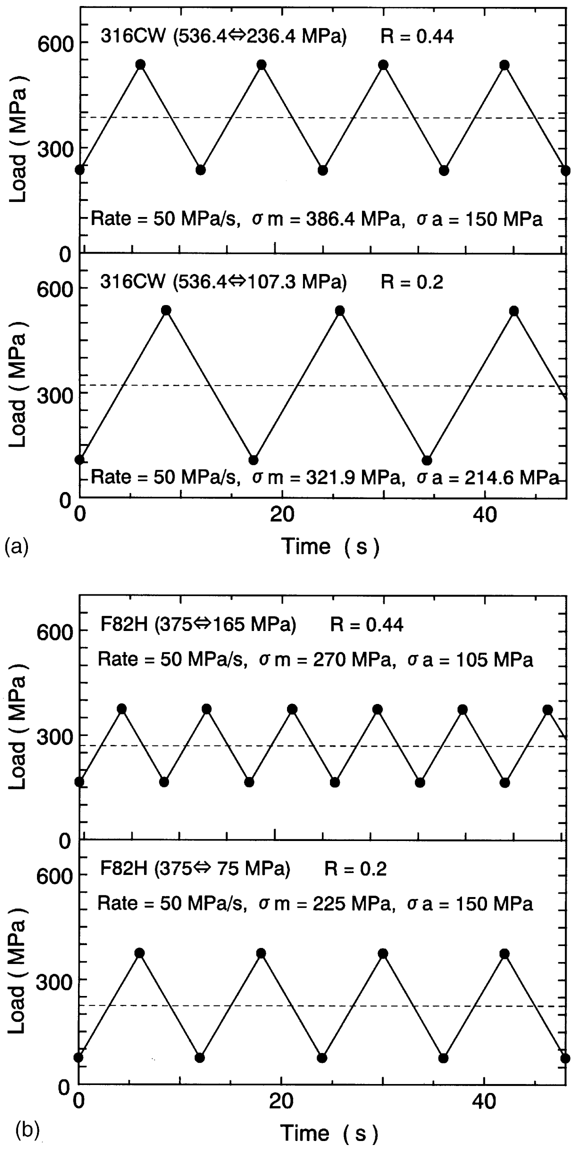

Fig. 2. Loading modes for (a) 316CW (20%CW-316SS, $\sigma_{max.} = 536.4$ MPa) and (b) F82H ($\sigma_{max.} = 375$ MPa).

fatigue tests, the fracture surfaces were examined by scanning electron microscopy (SEM, JEOL-5310).

3. Results and discussion

Table 2 summarizes the number of cycles to fracture (N_f) and the distance from the notch tip to the unstable fracture point on the fracture surface (a_{cr}) for all specimens. Table 2 shows that N_f was substantially increased under irradiation at $R = 0.44$ for both 316CW and F82H steels. This indicates the existence of the dynamic irradiation effect on fatigue response for both steels, irrespective of the difference in the crystal structure (fcc/bcc). However, at $R = 0.2$ where the higher loading amplitude was imposed on the specimens, N_f was similar for the in-beam and unirradiated specimens of both steels. The dynamic irradiation effect seems to be dependent on R, and it may decrease when the fatigue process proceeds faster at $R = 0.2$.

After the fatigue tests, the fracture surface was examined using SEM for all specimens. The macro-fractographic analyses of the fracture surface indicated some evidence of transgranular cracking in ductile fracture, namely, fibrous feature with some shear lips for all specimens. Fig. 3 presents the typical microscopic appearance on the fracture surface of the in-beam specimens of (a) 316CW and (b) F82H steels at $R = 0.44$. Fatigue striations were detected on fracture surface of all 316CW specimens, while striation-like markings with a number of secondary cracks were observed in all F82H specimens. Their characteristic appearance on fracture surfaces may reflect the difference in the crystal structures between 316CW (fcc) and F82H (bcc) steels. Much higher numbers of slip systems in bcc structures (24 compared to 12 in fcc structures) [9] may cause well-dispersed slips at the crack tip and hence lead to the formation of some complicated markings of striations with a number of secondary cracks on the fracture surface for F82H (bcc) steel. Larger capacity for cross slip due to higher stacking fault energy in bcc structures may also contribute to the complex trails of dislocation slips on the fracture surface of F82H steel. Either fatigue striations or striation-like markings were observed on the fracture surface in the area of crack growth from the notch tip until the critical point where unstable ductile fracture started. The value of a_{cr} shown in Table 2 is designated as the distance from the notch tip to the point where striations or striation-like markings disappear on the fracture surface. As presented in Table 2, the extension of N_f in the in-beam specimens at $R = 0.44$ was accompanied with the increase of a_{cr} for both steels. However at $R = 0.2$, the a_{cr} was similar for in-beam and unirradiated specimens of both steels. The increase in a_{cr} in the in-beam specimens at $R = 0.44$ may lead to the extended duration of the crack propagation process under irradiation and the subsequent extension of N_f for both steels. Since the value of a_{cr} reflects the materials resistance to the unstable ductile fracture [10], the dynamic irradiation effect appears to be associated with the increase in fatigue fracture toughness.

Table 2 also shows that there is a good agreement in the N_f values for the unirradiated specimens between 316CW steel at $R = 0.44$ and F82H steel at $R = 0.2$. The loading mode of 316CW at $R = 0.44$ has the higher average loading stress (σ_m) by 161.4 MPa but the same loading amplitude (σ_a) of 150 MPa as compared with the loading mode of F82H at $R = 0.2$, as shown in Fig.

Table 2
Experimental results of fatigue tests

	Loading mode	Irradiated condition	N_f	a_{cr} (μm)
316CW	$R = 0.44$ (536.4 $\Longleftrightarrow$ 236.4 MPa)	In-beam	10 364	902
		In-beam	12 050	805
		Unirradited	5243	684
		Unirradited	5362	608
		Unirradited	5510	680
	$R = 0.2$ (536.4 $\Longleftrightarrow$ 107.3 MPa)	In-beam	1812	654
		Unirradited	1780	633
F82H	$R = 0.44$ (375 $\Longleftrightarrow$ 165 MPa)	In-beam	36 141	797
		In-beam	28 743	767
		Unirradited	19 516	523
		Unirradited	19 080	582
	$R = 0.2$ (375 $\Longleftrightarrow$ 75 Mpa)	In-beam	6451	712
		In-beam	7131	716
		Unirradited	6787	687
		Unirradited	6643	654

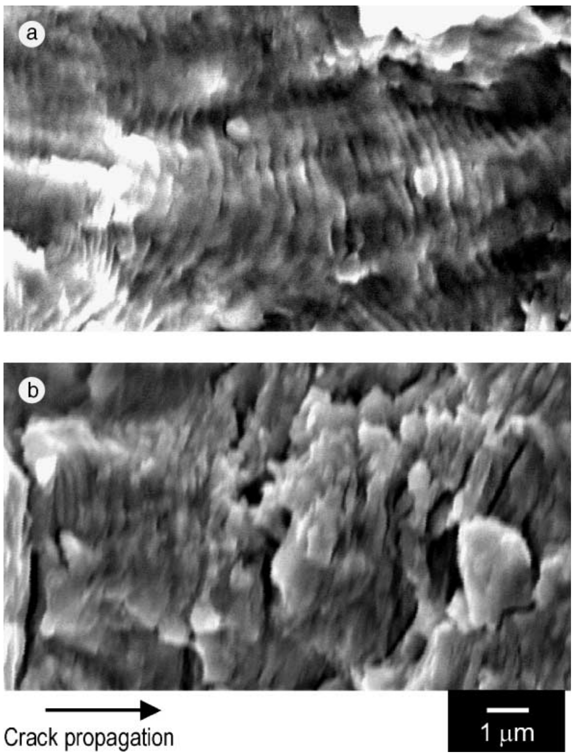

Fig. 3. Typical appearance of the fracture surface of the in-beam specimens at $R = 0.44$ for (a) 316CW and (b) F82H steels.

2(a) and (b). Since these two loading modes have the same period of 12 s/cycle, the general agreement in N_f suggests less significant difference in the actual lifetime of fatigue fracture between the two steels at the respective loading mode ($R = 0.44$ for 316CW and $R = 0.2$ for F82H) in the unirradiated condition. However, at the respective loading mode in the in-beam condition, the substantial extension of fatigue life was detected only for 316CW steel (see Table 2). This simply indicates that the fatigue response of F82H steel shows the lower sensitivity to the dynamic irradiation than that exhibited by 316CW steel. Since the interaction between continuously induced defect clusters and mobile dislocations has been considered as one of the key mechanisms of the dynamic irradiation effect on fatigue response [4,11], the intrinsic difference in stability of the radiation-induced defect clusters against gliding dislocations between 316CW (fcc) and F82H (bcc) steels would provide the sensitivity to the dynamic irradiation effect. An evidence of prismatic glide of the radiation-induced Frank loops in a bcc structure (molybdenum) [12] may support the lower sensitivity to the dynamic irradiation in F82H steel.

In the present experiments, slant fracture surfaces with an angle of 45° to the direction of applied stress (shear lips) were detected along the edges of the fracture surface for all specimens. The development of shear lips was more significant for F82H steel, and shear lips occurred at the longer distance from the notch tip on the fracture surface in the in-beam condition. The occurrence of shear lips on the fracture surface is often observed in thin sheets of materials with a bcc or fcc structure, and it is associated with the transition of the stressing state at the crack tip from plane strain condition to plane stress condition [13]. A possible alteration of crack growth rate accompanied with the occurrence of shear lips has been suggested in thin sheets of type 316 stainless steel [14]. Therefore, the effect of shear lips on the in-beam fatigue response will be further examined in the near future.

4. Conclusions

From the experimental results, the following conclusions (1)–(3) can be drawn:

(1) The number of cycles to fracture (N_f) was substantially increased under irradiation at $R = 0.44$ for both steels, while similar N_f was detected in both in-beam and unirradiated conditions at $R = 0.2$. This indicates the existence of the dynamic irradiation effect on fatigue response, irrespective of the crystal structure of the steels (fcc/bcc). The dynamic irradiation effect seems to be dependent on the applied loading ratio and it may decrease when the fatigue processes proceed faster.

(2) The increase in N_f in the in-beam specimens at $R = 0.44$ for both 316CW and F82H steels was accompanied by the extended area of crack growth on the fracture surface. The dynamic irradiation effect may be associated with the increase of fatigue fracture toughness.

(3) Although the actual lifetime of fatigue fracture was generally similar in the unirradiated specimens of 316CW steel at $R = 0.44$ and F82H steel at $R = 0.2$, the extension of fatigue life under the in-beam condition was detected only for 316CW steel at the respective loading mode. The lower sensitivity to the dynamic irradiation in F82H steel may reflect the difference in crystal structure between the two steels (fcc/bcc).

References

[1] T. Lechtenburg, J. Nucl. Mater. 133&134 (1985) 149.
[2] A. Kohyama, A. Hishinuma, D.S. Gelles, R.L. Klueh, W. Dietz, K. Ehrlich, J. Nucl. Mater. 233–237 (1996) 138.
[3] K. Shiba, A. Hishinuma, A. Tohyama, K. Masamura, JAERI-TECH. 97-038, 1997.
[4] R. Scholz, J. Nucl. Mater. 212–215 (1994) 546.
[5] P. Fenici, J. Nucl. Mater. 155–157 (1988) 963.
[6] Y. Murase, J. Nagakawa, N. Yamamoto, Y. Fukuzawa, ASTM STP 1366 (2000) 713.
[7] J. Nagakawa, Y. Murase, N. Yamamoto, Y. Fukuzawa, J. Nucl. Mater. 283–287 (2000) 391.
[8] Standard E 647-78T, Tentative test method for constant-load-amplitude fatigue-crack growth rates above 10^{-8} m/cycle, Annual Book of ASTM Standards, Part 10, Philadelphia, PA, 1978.
[9] J.C. Grosskreutz, ASTM STP 495 (1971) 5.
[10] V.T. Troshchenko, V.V. Pokrovsky, P.V. Yasniy, Fatigue Fract. Eng. Mater. Struct. 17 (1994) 991.
[11] R. Tulluri, D.J. Morrison, J. Mater. Eng. Perform. 6 (1997) 454.
[12] M. Suzuki, A. Fujimura, A. Sato, J. Nagakawa, N. Yamamoto, H. Shiraishi, Philos. Mag. A. 64 (1991) 395.
[13] J. Zuidema, J.P. Krabbe, Fatigue Fract. Eng. Mater. Struct. 20 (1997) 1413.
[14] D.G. Rickerby, P. Fenici, Eng. Fract. Mech. 19 (1984) 585.